Zespół Teoretycznego Modelowania Procesów Chemicznych

Wydział Chemii

Uniwersytet Wrocławski

Sprawozdanie za 2011 rok

Skład Zespołu:

prof. dr hab. Zdzisław Latajka - kierownik Zespołu

dr hab. Jerzy Moc – adiunkt

dr hab. Robert Wieczorek – adiunkt

dr Sławomir Berski - adiunkt

dr Małgorzta Biczysko

dr Andrzej Bil – adiunkt

dr Przemysław Dopieralski - adiunkt

dr Piotr Durlak - adiunkt

dr Krzysztof Mierzwicki - adiunkt

dr Jarosław Panek – adiunkt

mgr Monika Borkowska-Panek - doktorantka

mgr Emilia Makarewicz - doktorantka

mgr Piotr Okrasiński – doktorant

mgr Paweł Panek – doktorant

mgr Nuno Manuel Almeida Barbosa – doktorant

mgr Łukasz Fojcik - stażysta

Realizowane projekty badawcze

Badania kwantowomechaniczne tlenków i ozonków fulerenu C_{70} i ich modyfikowanych endohedralnie analogów.

Projekt badawczy własny, nr. N N204 2807 38

Realizacja projektu: 29.03.2010 – 28.03.2013

Kierownik: dr Andrzej Bil

Próba wyjaśnienia natury oddziaływań oraz opis struktury geometrycznej i elektronowej układów wielodziałowych zaangażowanych w tworzenie nietypowych kompleksów molekularnych.

Projekt badawczy własny, nr. N N204 3061 37

Realizacja projektu: 01.10.2009 -31.09.2011

Kierownik: dr Jarosław Panek

Eksperymentalne i teoretyczne badania układów oddziaływujących z ksenonem oraz zmian struktury układów molekularnych indukowanych światłem podczerwonym w niskich temperaturach (XEPHOT).

Międzynarodowy projekt badawczy w ramach konkursu ERA Chemistry, Open Initiative 2009;

nr. projektu: ERA-Chemistry-2009/01/2010

Realizacja projektu: 25.01.2011 – 24.01.2014

Kierownik: prof. dr hab. Zdzisław Latajka

Wynik realizacji grantu obliczeniowego:

25 *prac opublikowanych w czasopismach międzynarodowych*
(sumaryczny ImpF = ***74,564****, Pkt. =* ***759****)*

19 *wystąpień konferencyjnych na konferencjach międzynarodowych (w tym 6 wykładów)*

6 *obronionych prac magisterskich*

Teoretyczne modelowanie własności układów i procesów chemicznych

Angewandte Chemie

Enforced Ring-Opening

DOI: 10.1002/ange.201100399

Force-Transformed Free-Energy Surfaces and Trajectory-Shooting Simulations Reveal the Mechano-Stereochemistry of Cyclopropane Ring-Opening Reactions**

Przemyslaw Dopieralski, Jordi Ribas-Arino,* and Dominik Marx*

Angew.Chem.Int.Ed., 123 (2011) 7243 – 7246

Mechanochemistry of 1,1-dichloro-2,3-dimethylcyclopropane

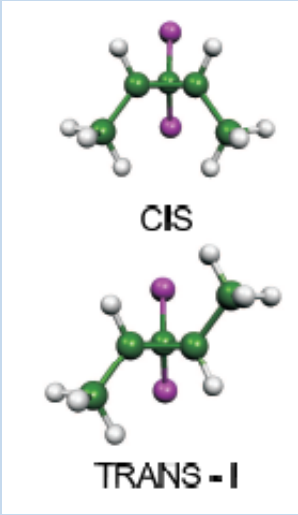

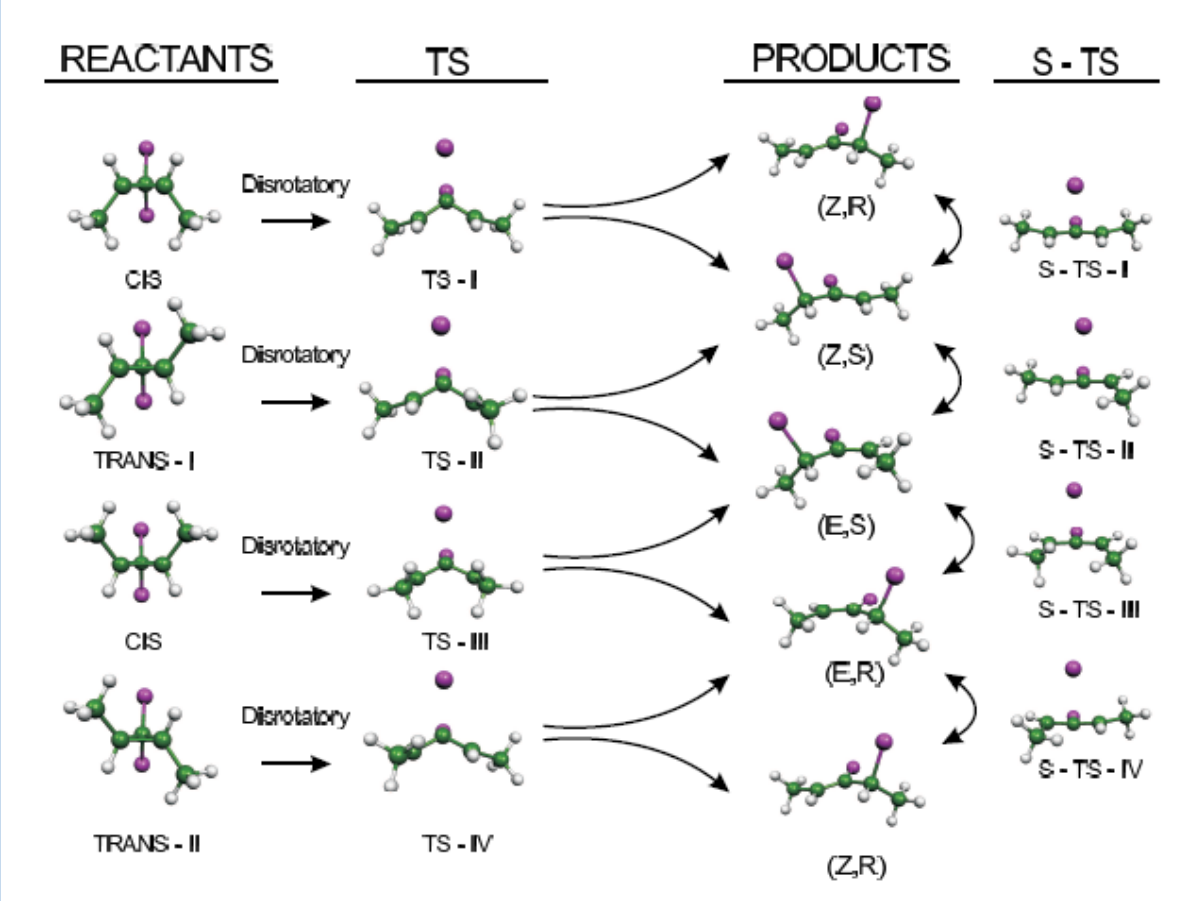

FIG. 1: Scheme showing the involved chemical species, i.e. all reactants (cis; trans–I and trans–II being enantiomers), transition states (TS–I to TS–IV; S–TS–I to S–TS–IV), and products (Z,R; Z,S; E,S; E,R). The arrows connecting the reactants with the distinct products via the corresponding TSs represent the reaction paths obtained from IRC mapping and ab initio trajectory shooting starting from the TSs (see text). The second set of TSs (S–TS) belongs to interconversion reactions between selected products as indicated. For simplicity all structures correspond to the stationary points at zero force, the Z,R product is reproduced twice for clarity, and the Cl atoms are colored violet.

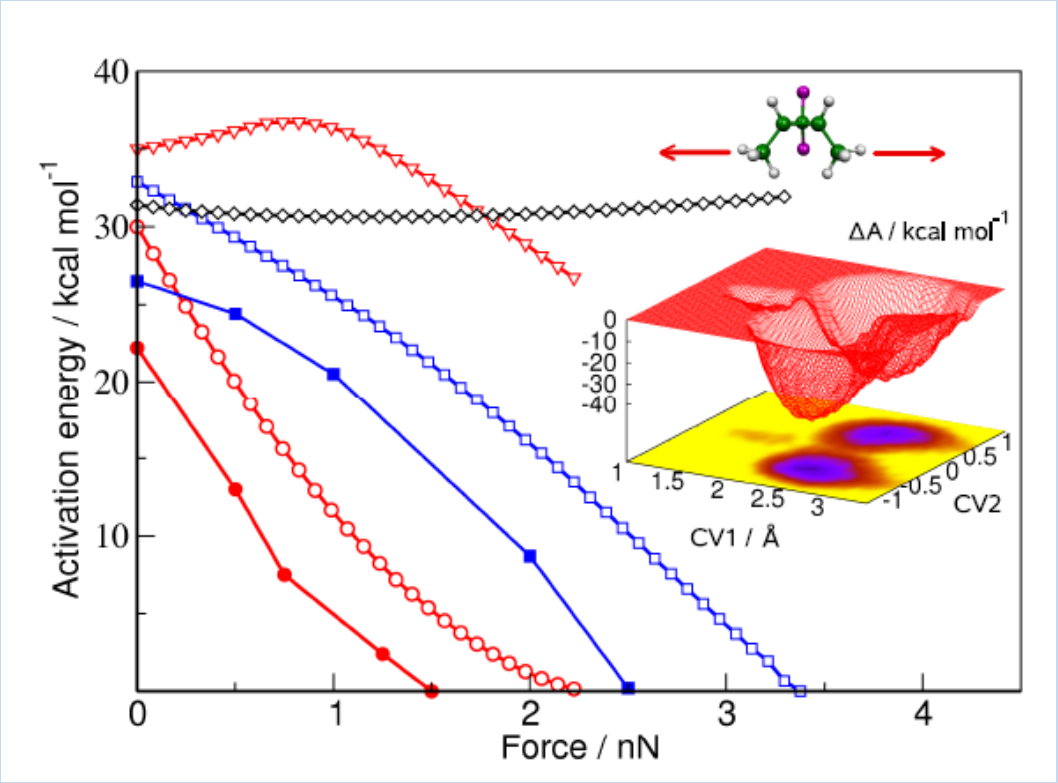

FIG. 3: Force–dependence of activation energies $\Delta E^{\ddagger}(F_0)$ (open symbols) and free energies $\Delta A^{\ddagger}(F_0)$ at 300 K (filled symbols) of the disrotatory ring–opening of cis (red circles for the "outward" pathway; red triangles for "inward" pathway) and trans (blue squares) 1,1–dichloro–2,3–dimethylocyclopropanes. The force–dependence of $\Delta E^{\ddagger}(F_0)$ for the interconversion between Z,R and Z,S products is also depicted (black diamonds). The stretching force is applied to the C atoms of the two terminal methyl groups (see Figure 1) as indicated in the upper inset. Large inset: Force–transformed free energy landscape for ring–opening of cis reactant at a constant external force of $F_0 = |\mathbf{F}_0| = 1.25$ nN. These FT–FESs have been obtained in a reaction subspace spanned by two collective variables: CV1 is the C$\cdots$C distance associated with the bond that yields upon the ring–opening process. CV2 is the difference $CN_1 - CN_2$ of the coordination numbers of both chlorine atoms with respect to the left (CN_1) or right (CN_2) carbon atom in the cyclopropane ring.

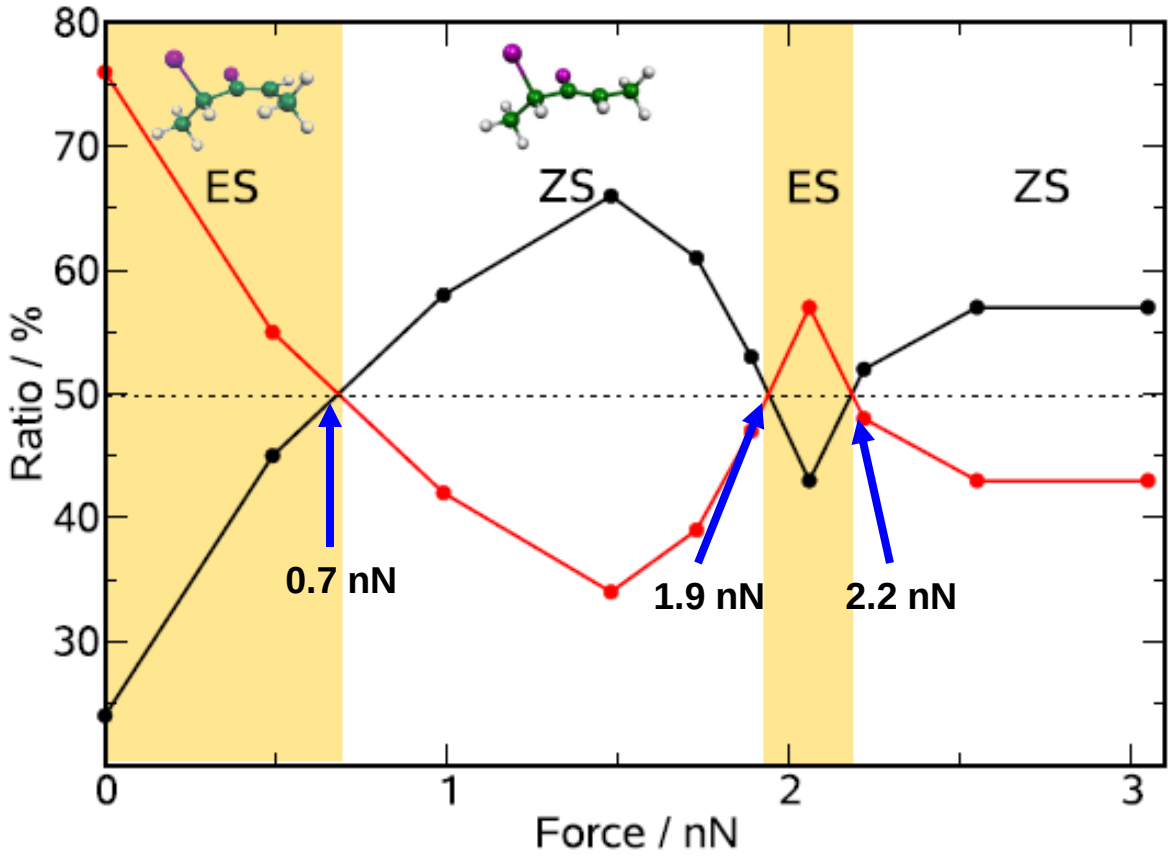

FIG. 4: Force–dependence of the probability of obtaining the E,S–products (red) versus Z,S–products (black) upon ring–opening of trans reactant as computed from dynamical trajectory shooting simulations. The range of forces with yellow and white backgrounds correspond to the forces at which the majority product of the ring–opening process is the E,S–alkene or the Z,S–alkene, respectively.

Short, low-barrier H-bonds (LBHBs)

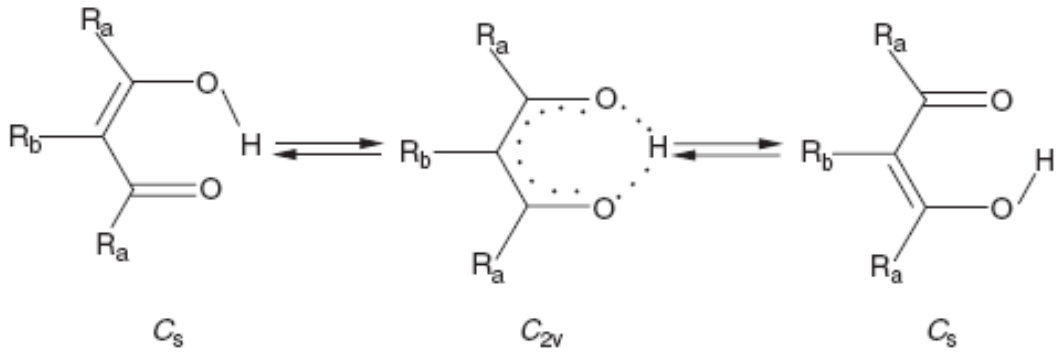

Figure 4. Tautomeric conformations of β-diketones.

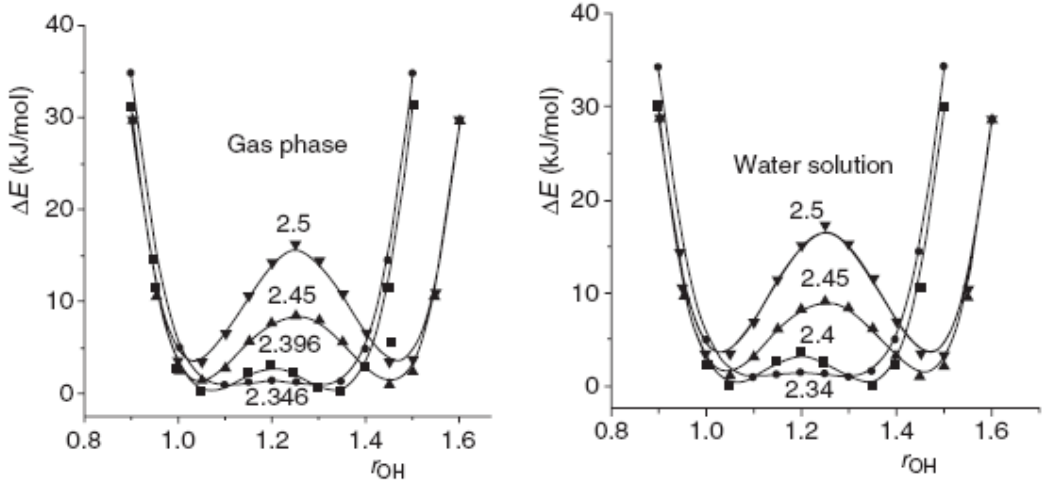

Figure 5. Potential energy curves versus r_{O-H} in vacuum and in water solution for some frozen $r_{O\cdots O}$ values of nitromalonamide. (Reprinted from Ref. 159 with permission from Elsevier.)

From:

G.Buemi, in „Hydrogen Bonding – New Insights”, Ed. S.Grabowski, Springer, 2006, pp. 51-107

Problem – the symmetry of short, low-barrier H-bonds in solution

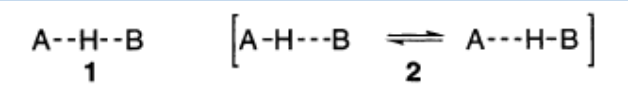

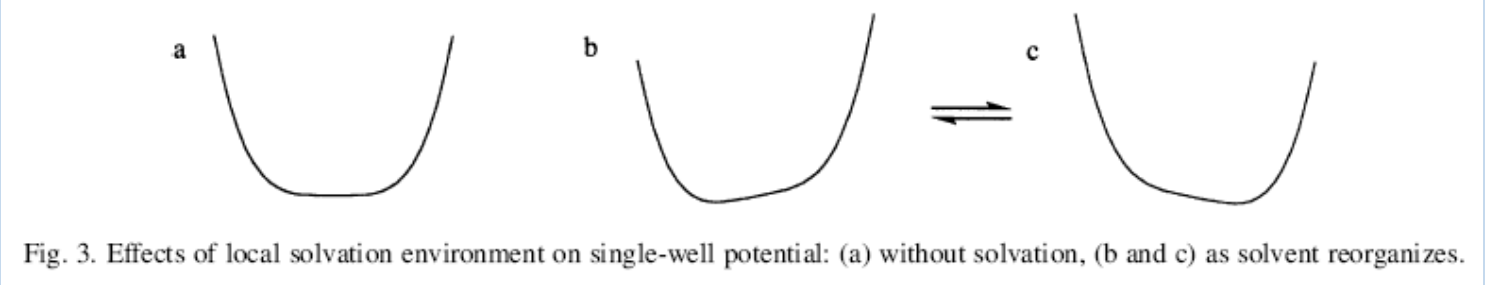

Fig. 3. Effects of local solvation environment on single-well potential: (a) without solvation, (b and c) as solvent reorganizes.

In solution – equilibrium between solvatomers.

C.L. Perrin, Pure Appl.Chem., 81 (2009) 571 – 583

C.L. Perrin, Acc.Chem.Res., 43 (2010) 1550 – 1557

Hydrogen maleate anion

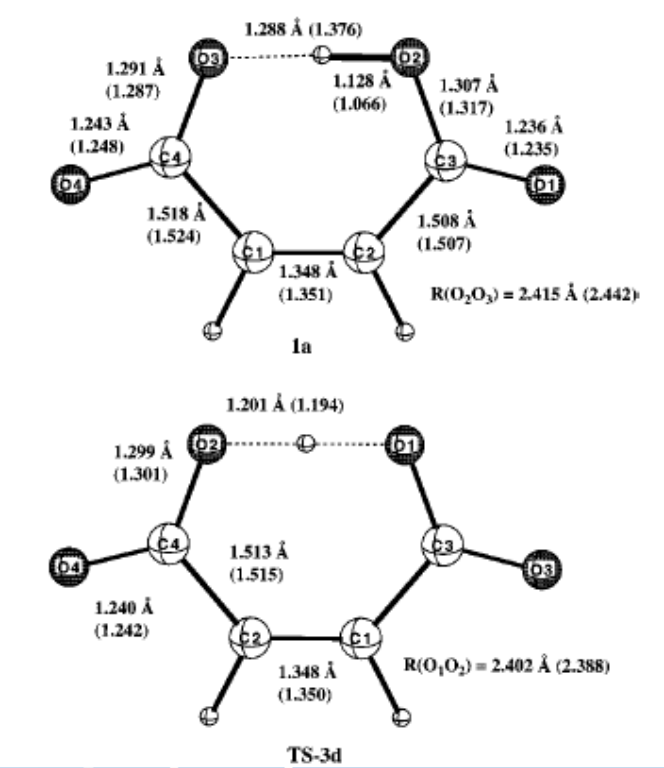

R.D.Bach, O. Dmitrenko, M.N. Glukhovtsev, J.Am.Chem.Soc., 123 (2001) 7134

QCISD(T)/6-311++G(d,p)//QCISD/6-31+G(d,p)

Barrier 0.2 kcal/mol

H.-K. Woo, X.-B. Wang, L.-S. Wang, K.-C. Lau, J.Phys.Chem. A, 109 (2005) 10633

Estimated intramolecular hydrogen bond strength - 21.5 2.0 kcal/mol

J.Chem.Theor.Compt., 7 (2011) 3505-3513

JCTC Journal of Chemical Theory and Computation

ARTICLE

pubs.acs.org/JCTC

On the Intramolecular Hydrogen Bond in Solution: Car−Parrinello and Path Integral Molecular Dynamics Perspective

Przemyslaw Dopieralski,*,† Charles L. Perrin,*,‡ and Zdzislaw Latajka†

†Faculty of Chemistry, University of Wroclaw, Joliot−Curie 14, 50-383 Wroclaw, Poland

‡Department of Chemistry and Biochemistry, University of California at San Diego, La Jolla, California 92093-0358, United States

Supporting Information

CPMD, PIMD, 298K

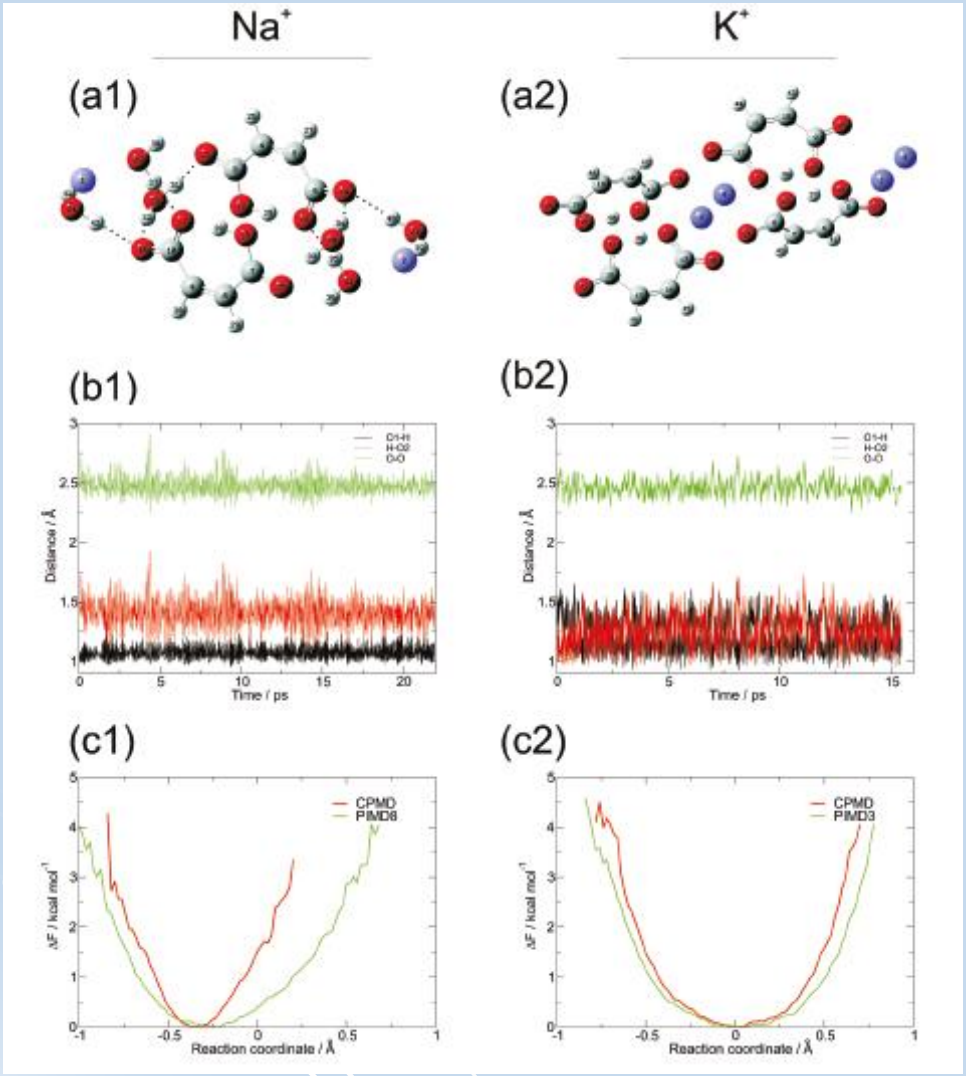

Table 1. Time-Averaged Intramolecular H-bond Distances from Calculations on Sodium and Potassium Hmaleate Salts

	NaHMal			KHMal	
bond	CPMD	PIMD8	expt[14]	CPMD	expt[36]
O–H	1.08	1.13	1.079	1.22	–
H···O	1.41	1.37	1.369	1.23	–
O···O	2.48	2.47	2.445	2.44	2.434

KHMal 1.2 0.1 Å

...K^+...O1 – H – O2...K^+....

Isolated Hmal O...O 2.457 Å, O...H 1.235 Å

Hydrogen maleate ion in water (103 molecules)

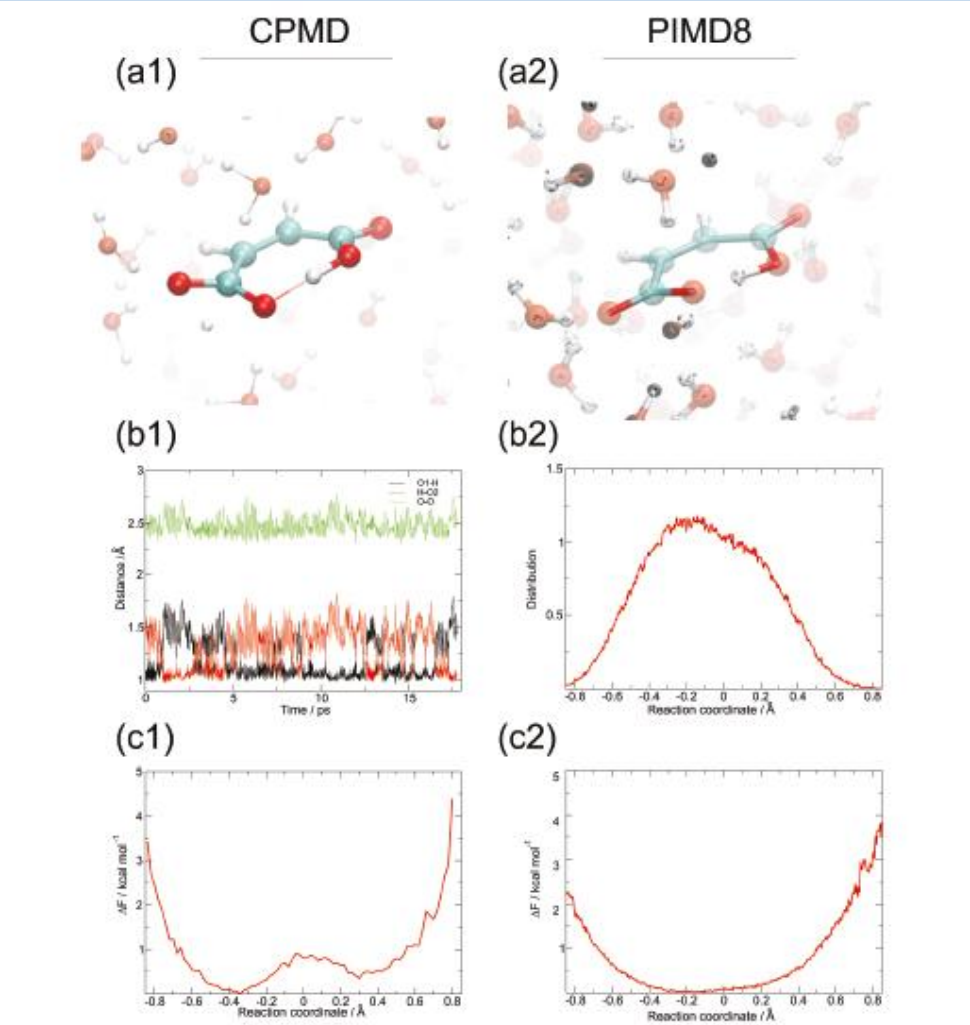

Figure 2. Hmaleate ion in water from CPMD (left column: a1, b1, and c1) and from PIMD (right column: a2, b2, and c2). (a1,a2) Representative snapshot from simulations, for PIMD the replicas of each atom as small gray spheres are marked. (b1) Time evolution of the distances involved in the intramolecular H-bond. (b2) Distribution function for the reaction coordinate (c1,c2) Free energy profiles for proton transfer within the H-bond.

	CPMD	PIMD
O1-H...O2	48.2%	44.6%
O1...H-O2	15.1%	16.5%
O1...H...O2	36.7%	38.9%

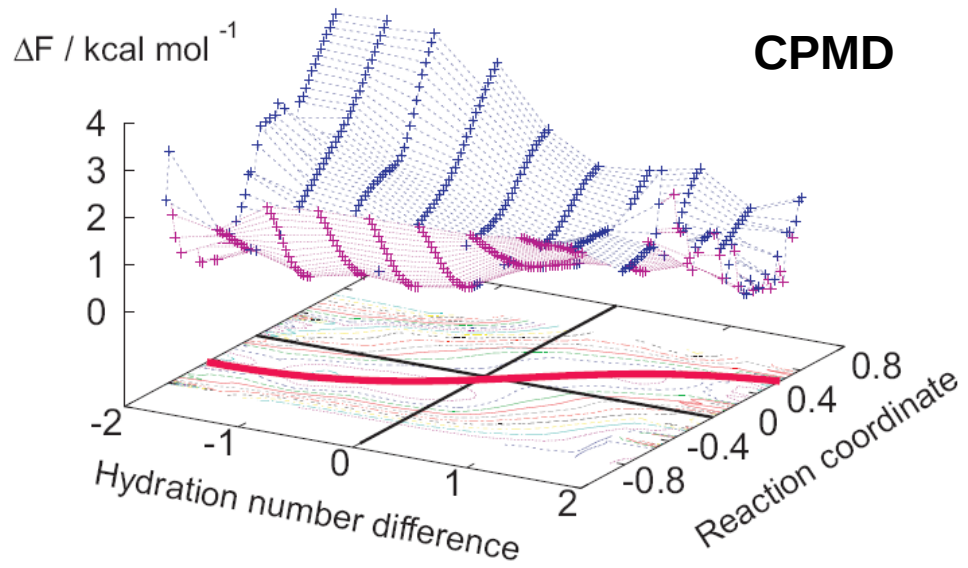

Figure 1: Car–Parrinello free-energy profile for Hmaleate anion in water. Red solid line indicates minimum free energy pathway.

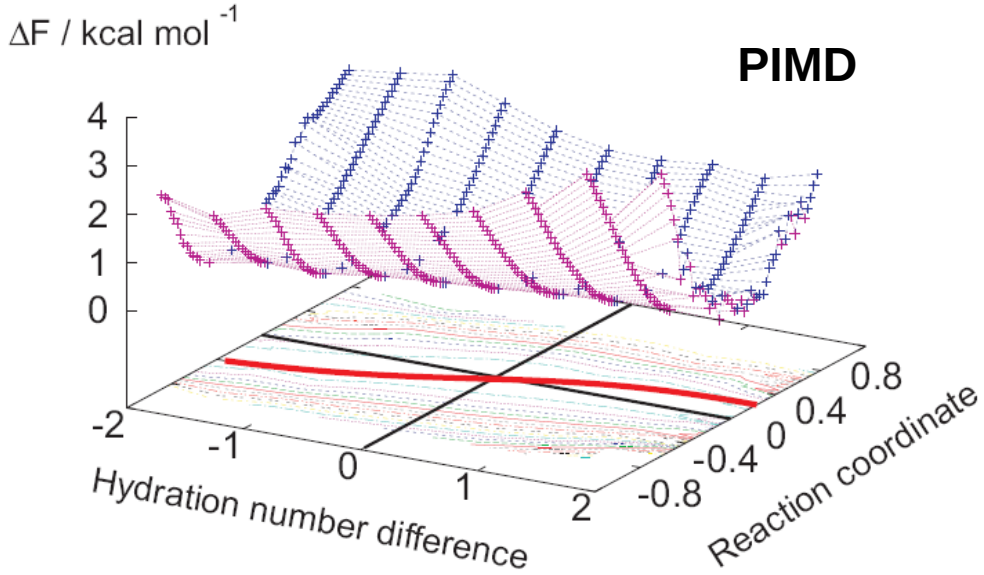

Figure 2: Path Integral free-energy profile for Hmaleate anion in water. Red solid line indicates minimum free energy pathway.

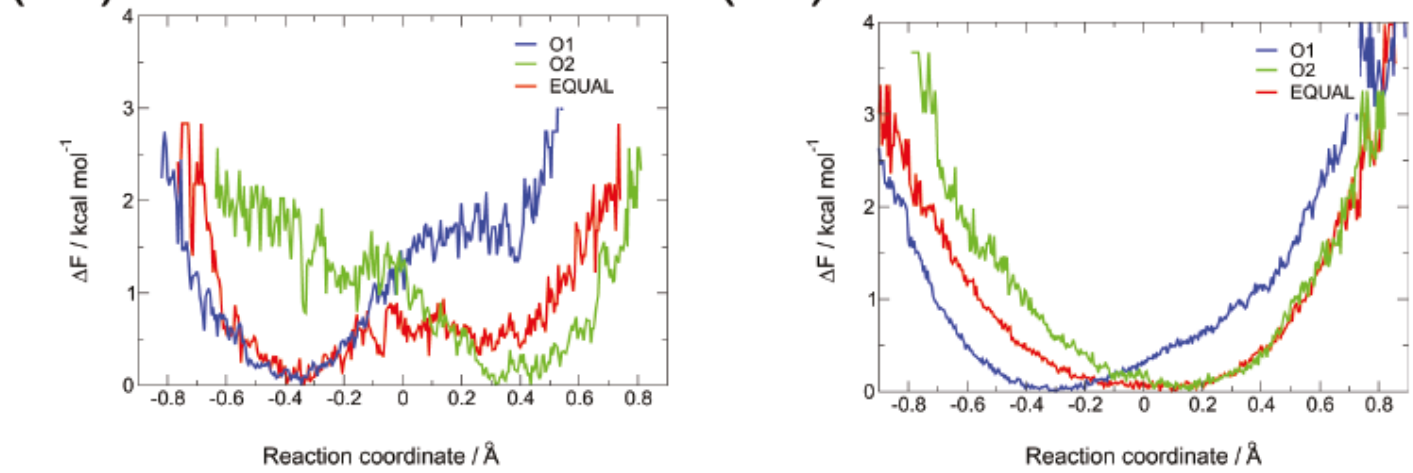

Figure 3. Free-energy profiles for H motion in aqueous Hmaleate ion from CPMD (a1) and from PIMD (a2) separately for the simulation time when O1 was less solvated than O2, for the time when O2 was less solvated than O1, and for the time when both oxygen atoms were solvated similarly.

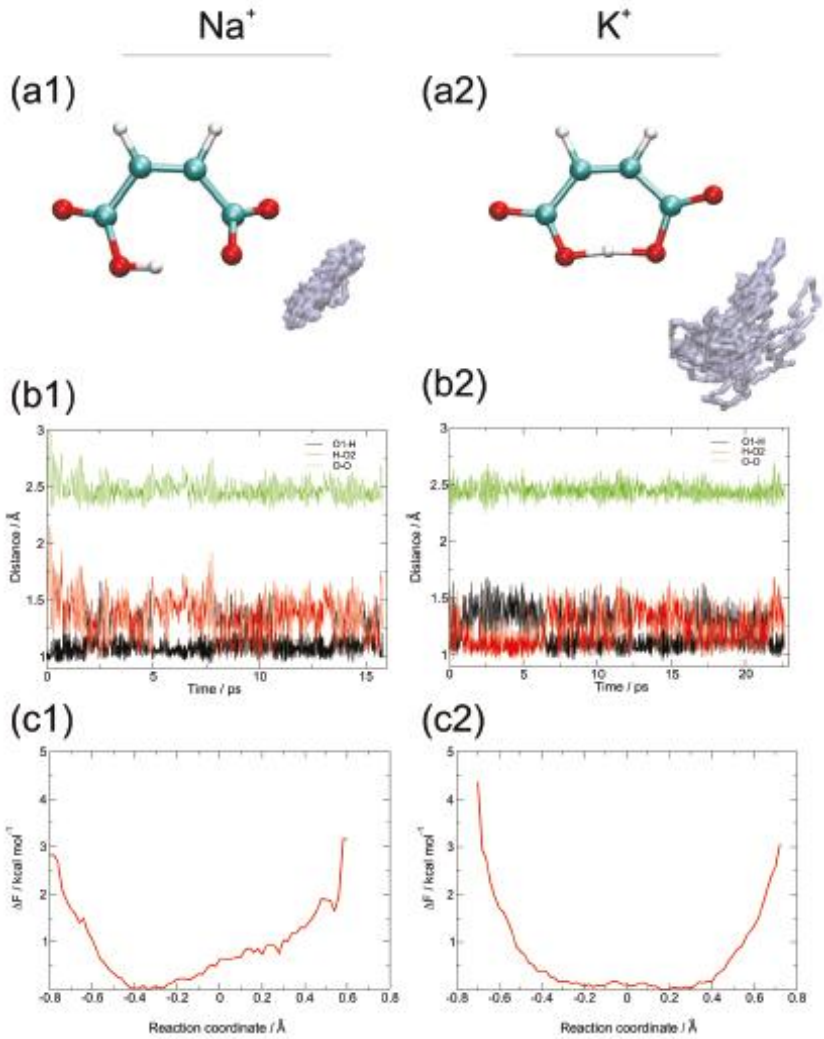

Figure 4. Hmaleate ion in water from CPMD simulations with two different counterions: sodium (left panel: a1, b1, and c1) and potassium (right panel: a2, b2, and c2). (a1,a2) Spatial distribution function of the counterion around Hmaleate ion. (b1,b2) Time evolution of the O−H distances involved in the intramolecular H-bond. (c1,c2) Free-energy profile for proton transfer within the H-bond.

NaHMal and 102 H_2O

KHMal and 101 H_2O

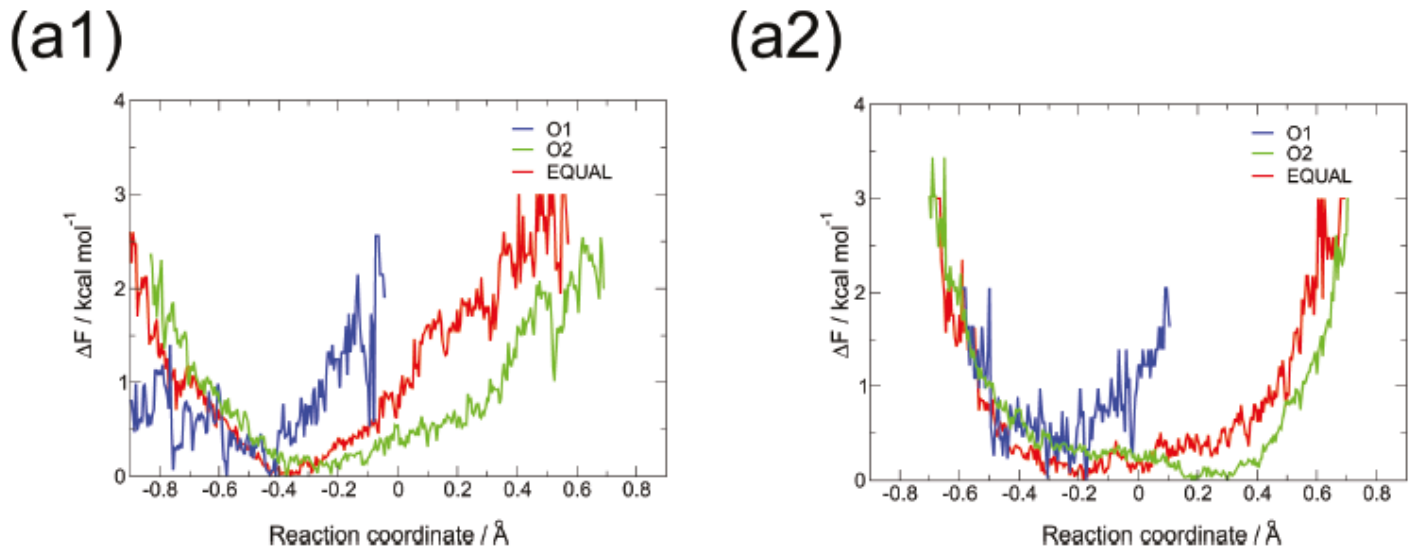

Figure 5. CPMD free-energy profiles for Hmaleate anion with Na^+ (a1) and K^+ (a2) separately for the simulation time when O1 was less solvated than O2, for the time when O2 was less solvated than O1, and for the time when both oxygen atoms were solvated similarly.

Chemical Physics Letters 514 (2011) 44–48

Contents lists available at SciVerse ScienceDirect

Chemical Physics Letters

journal homepage: www.elsevier.com/locate/cplett

Reinvestigation of spectroscopic properties for ammonia–hydrogen halide complexes from Car–Parrinello Molecular Dynamics

Paweł Panek [a,*], Malgorzata Biczysko [b], Zdzisław Latajka [a]

[a] Faculty of Chemistry, University of Wrocław, F. Joliot-Curie 14, 50-383 Wrocław, Poland
[b] Dipartimento di Chimica 'Paolo Corradini' and INSTM M3-Village Università di Napoli Federico II, Complesso Univ. Monte S. Angelo, via Cintia, 80126 Napoli, Italy

P. Goldfinger, G. Verhaegen, J.Chem.Phys., 50 (1960) 1467 (high temperature mass spectroscopy)

B. Ault, G. Pimentel, J.Phys.Chem., 77 (1973) 705 (matrix isolation IR spectra)

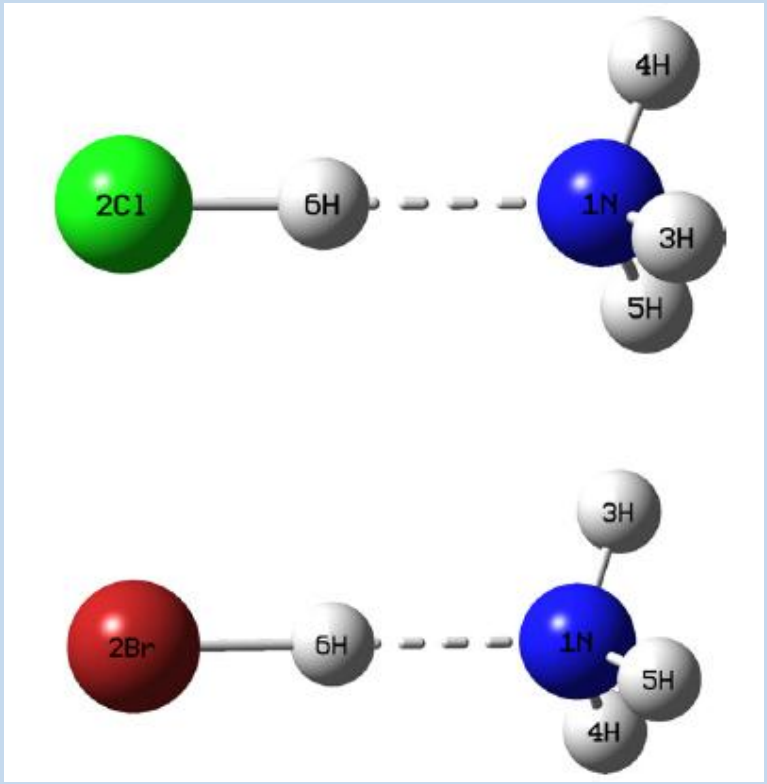

CPMD 100K 35ps simulation BLYP

MP2, BLYP, B3LYP VSCF, VPT2

Predictions: A. Barnes, Z. Latajka, M. Biczysko, J.Mol.Struct., 614 (2002) 11

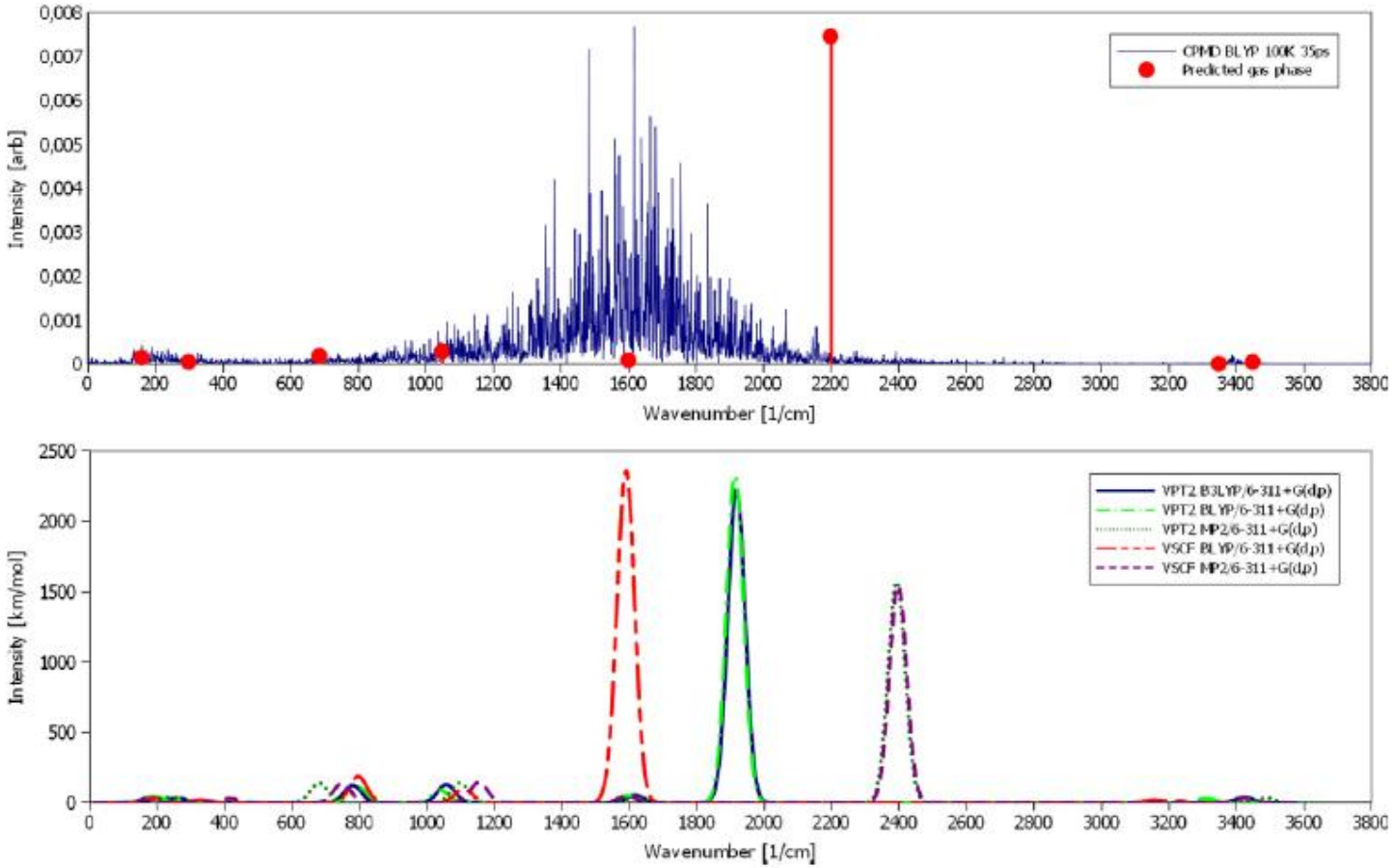

Figure 2. Cl–H···NH_3 vibrational spectra obtained from Car–Parrinello Molecular Dynamics (upper) as well as from VPT2 and VSCF vibrational frequencies calculations (lower). Predicted gas phase stick spectrum, for sake of comparison, has been composed of predicted vibrational frequencies for gas phase (see Ref. [29]) and calculated harmonic IR intensities at BLYP/6-311+G (d,p) level.

H-Cl str. MP2: VSCF, VPT2 ~2400 cm^{-1}; BLYP: VSCF ~1600 cm^{-1}

BLYP, B3LYP: VPT2 ~1600 cm^{-1}

Predictions: A. Barnes, Z. Latajka, M. Biczysko, J.Mol.Struct., 614 (2002) 11

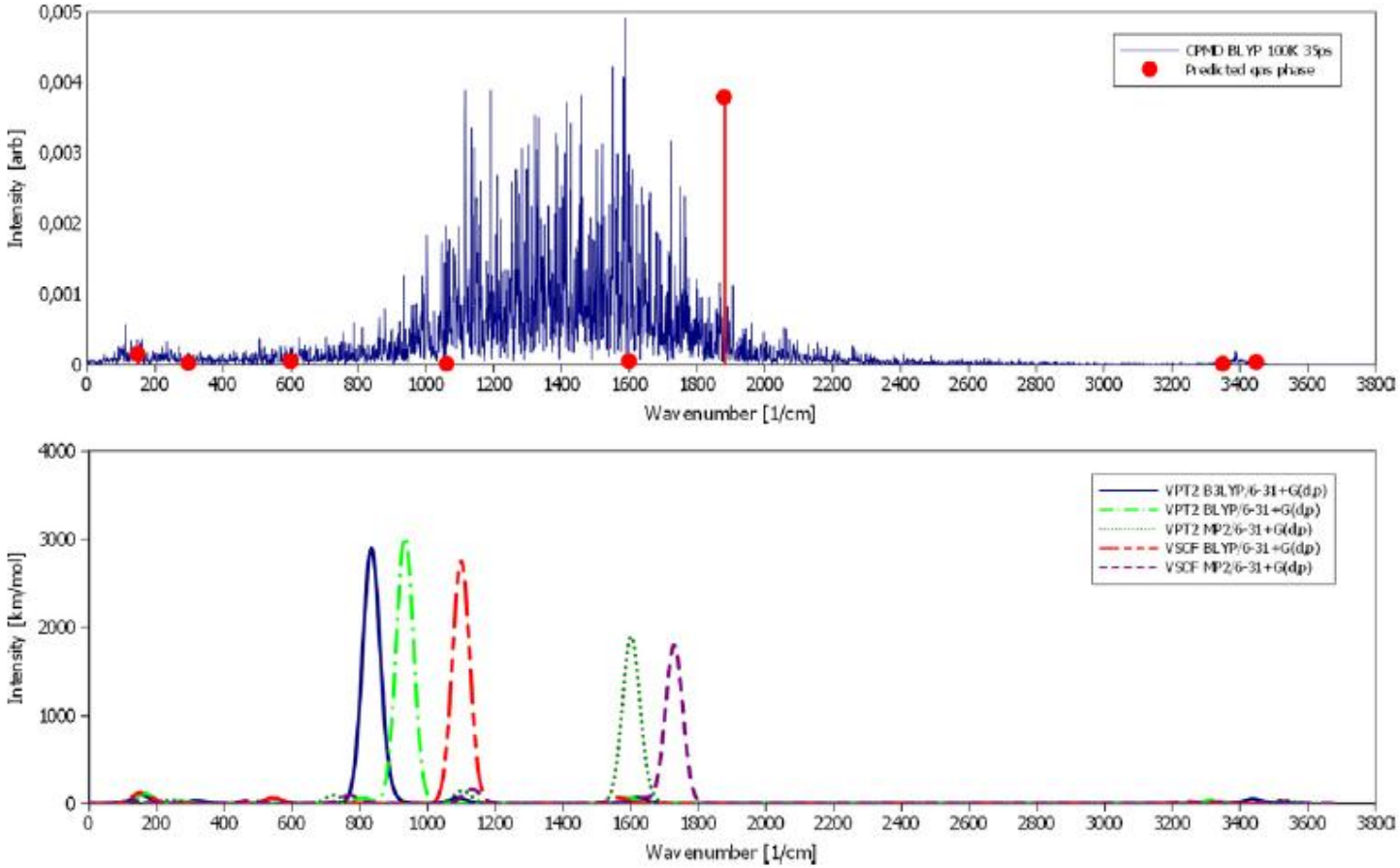

Figure 3. Br–H···NH_3 vibrational spectra obtained from Car–Parrinello Molecular Dynamics (upper) as well as from VPT2 and VSCF vibrational frequencies calculations (lower). Predicted gas phase stick spectrum, for sake of comparison, has been composed of predicted vibrational frequencies for gas phase (see Ref. [29]) and calculated harmonic IR intensities at BLYP/6-31+G (d,p) level.

H-Br str. MP2: VSCF ~1600 cm-1, VPT2 ~1750 cm^{-1}; B3LYP: VPT2 950 cm^{-1}

BLYP: VSCF ~1100 cm^{-1} VPT2 ~850 cm^{-1}

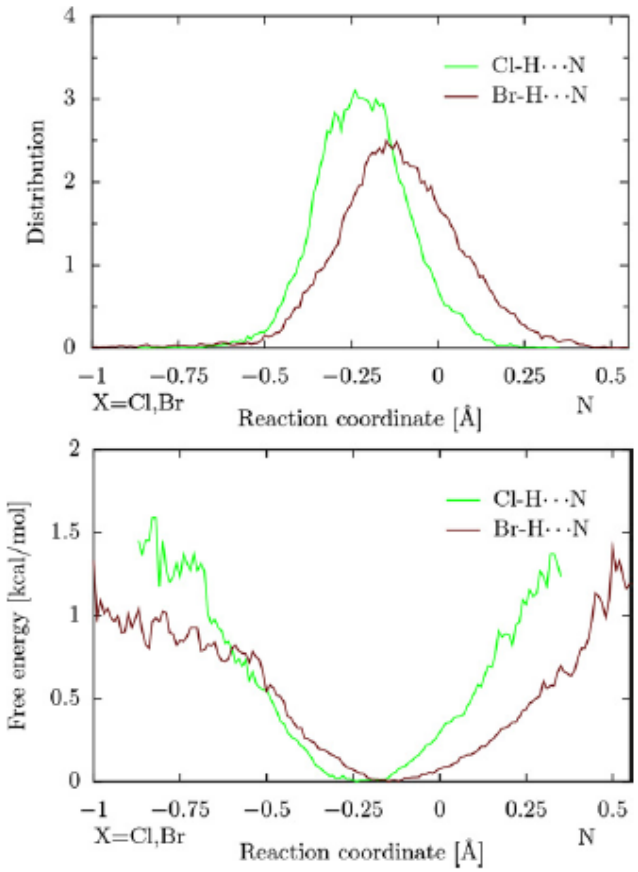

Figure 4. Proton distribution along X–H···N coordinate within the simulation (upper) and proton transfer free energy given in kcal/mol along X–H···N obtained from proton distribution (lower).

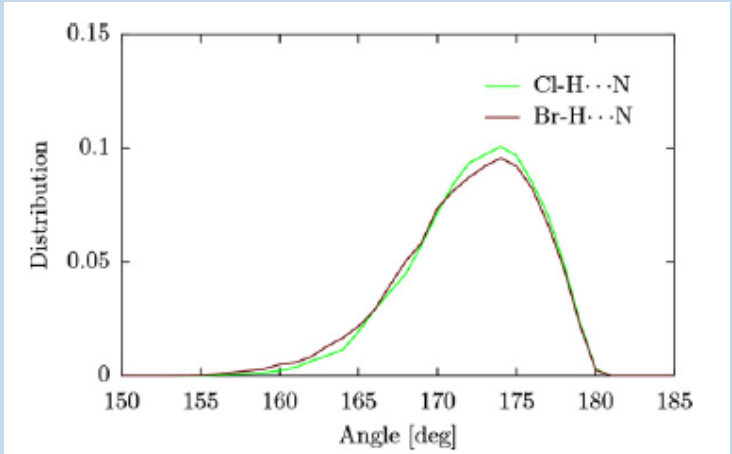

Figure 5. X–H···N angle distribution within the simulation.

Suggested the gas phase values of proton stretching frequencies:

Cl – H....N 1750 cm^{-1} and Br – H ...N 1550 cm^{-1}

Topological analysis of ELF

The gradient field of ELF → **basins**

Types of basins:

- **core basins – C**
- **valence basins – V**

synaptic order	nomeclature	symbol
1	monosynaptic	$V(X_i)$
2	disynaptic	$V(X_i,Y_j)$
≥3	polysynaptic	$V(X_i,Y_j,\ldots)$

Average population: $\tilde{N}(\Omega_A) = \int_{\Omega A} \rho(r)\, d(r)$

Fluctuation (variance) in the mean number of electrons in a basin

$$\sigma^2(\tilde{N},\Omega) = \langle N^2\rangle_\Omega - \langle N\rangle^2_\Omega$$

measure of delocalization

ELF - population rules

V(C)	**≥ Z - N_v**	**increase with Z**
V(X)	**~ 2.0**	**lone pair**
V(X,Y)	**< 2.0**	**single bond**
V(X,H)	**1.5 2.5**	**X-H bond**

Charge-shift bond -> Protocovalent bond

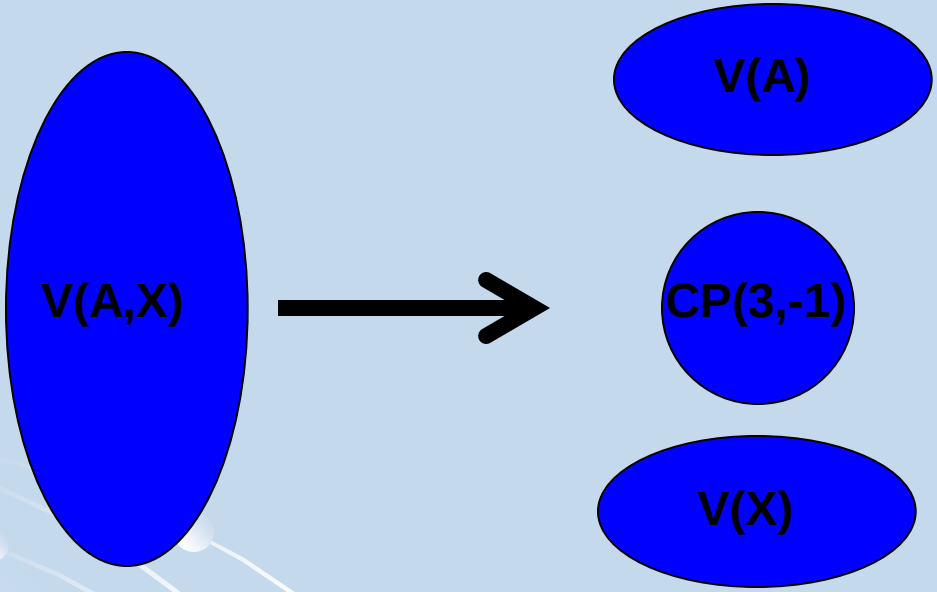

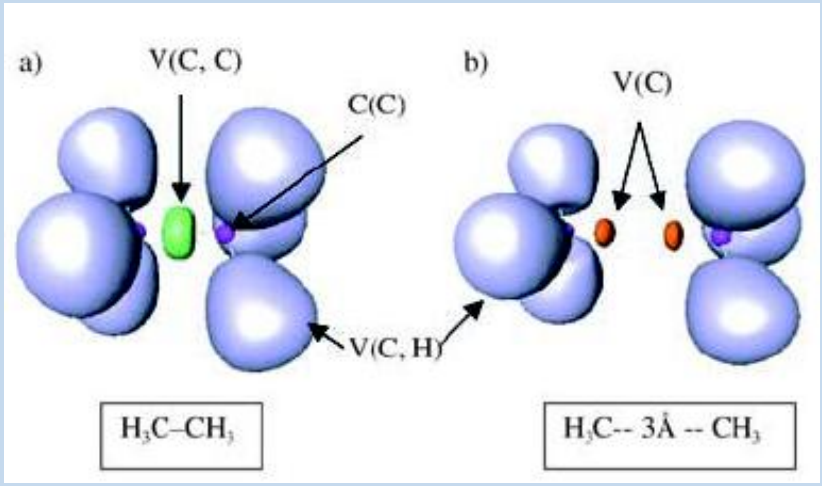

- **Populations of monosynaptic basins on the intermolecular axis are very small.**
- **Large exchange electrons between two basins.**

Nitrous acid HONO

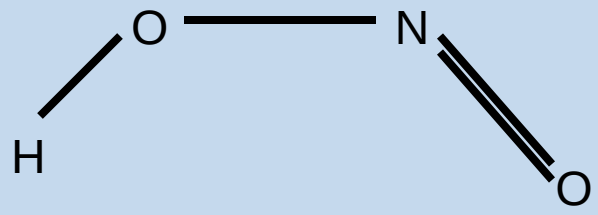

HONO-cis

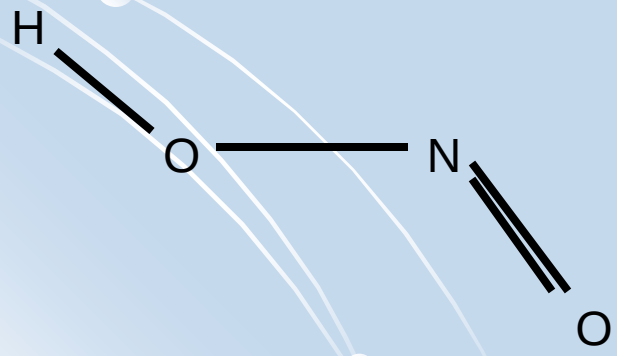

HONO-trans

Nitrous acid HONO – ELF picture of bonds

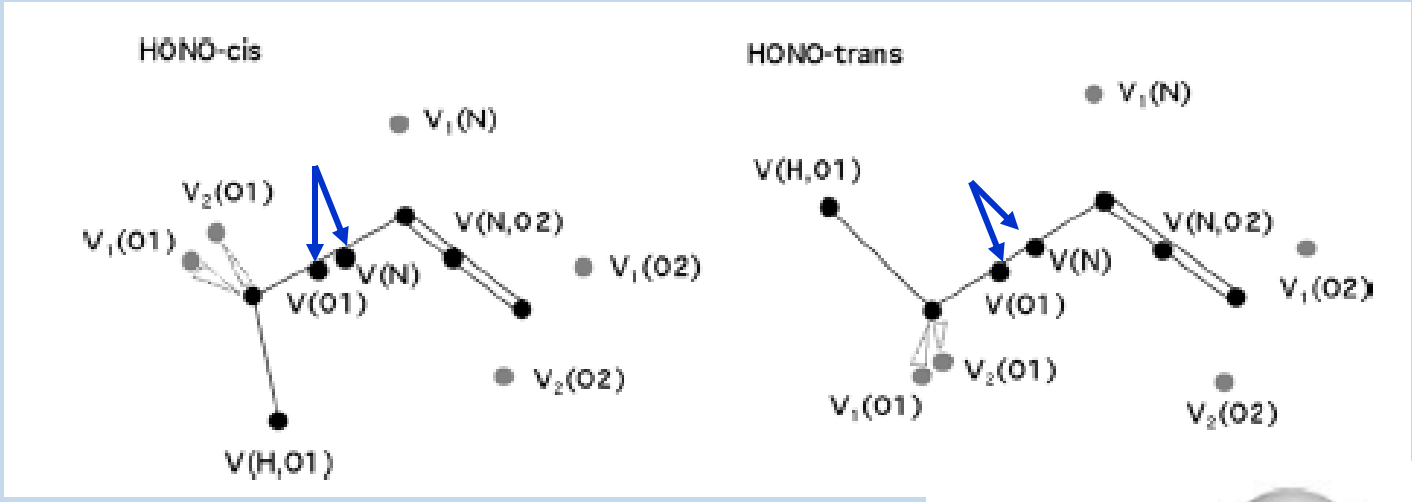

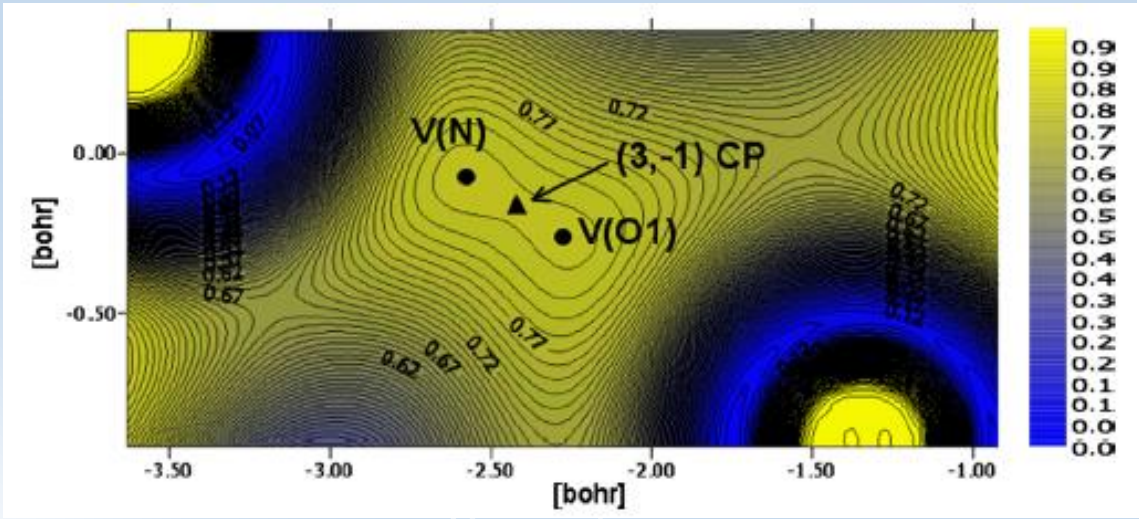

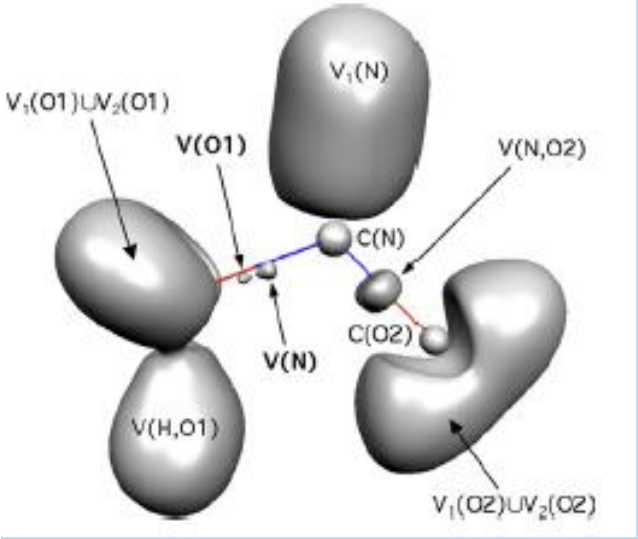

HONO-cis, ELF

CASSCF(12,10)/6-311++G(2d,2p)

ELI-D

S.Berski, K.Mierzwicki, A.Bil, Z.Latajka, Chem.Phys.Lett., 460 (2008) 559

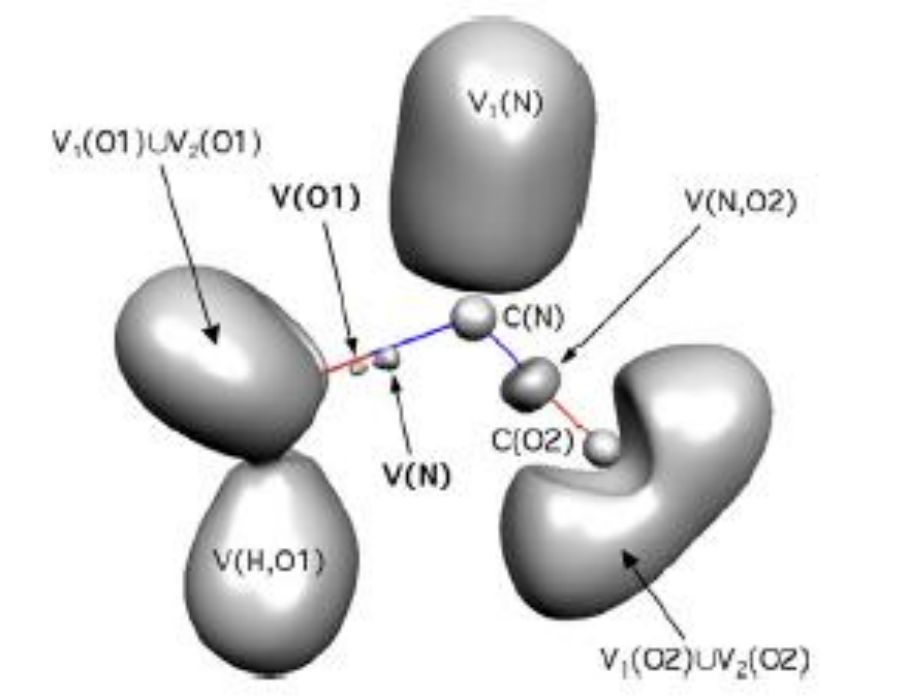

V(O1)	*0.39 e*	*trans*
V(N)	*0.53 e*	
V(N,O2)	2.03 e	

V(O1)	*0.47 e*	*cis*
V(N)	*0.61 e*	
V(N,O2)	1.95 e	

V(N,O)	1.67 e	NO_2
V(N,O)	1.53 e	NO_2^+
V(N,O)	1.82 e	NO_2^-

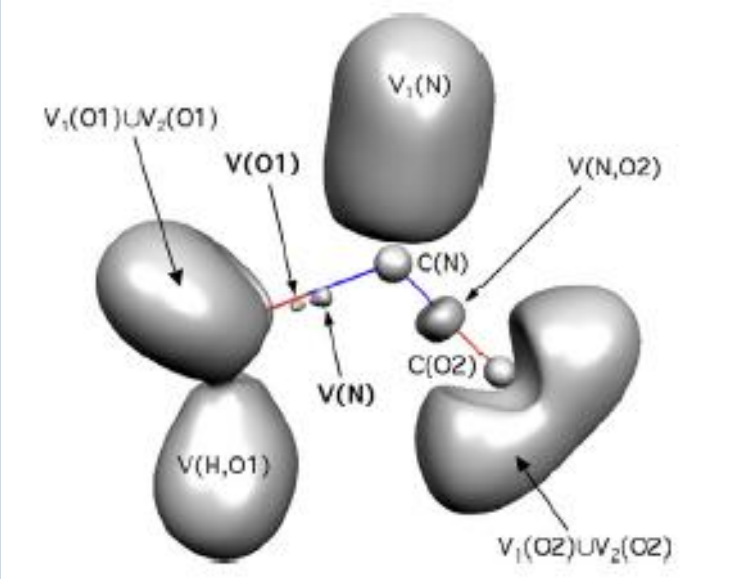

$HONO(^1A') \rightarrow OH(^2\pi) + NO(^2\pi)$ $\Delta H^o_0 = 48.0$ kcal/mol

$HONO(^1A') \rightarrow OH(^2\Sigma) + NO(^2\pi)$ $\Delta H^o_0 = 140.6$ kcal/mol

$HONO(^1A') \rightarrow H(^2S) + NO_2(^2A_1)$ $\Delta H^o_0 = 77.5$ kcal/mol

$HONO(^1A') \rightarrow H(^2S) + NO_2(^2B_2)$ $\Delta H^o_0 = 105.3$ kcal/mol

$HONO(^1A') \rightarrow H(^2S) + NO_2(^2B_1)$ $\Delta H^o_0 = 117.9$ kcal/mol

$HONO(^1A') \rightarrow H(^2S) + NO_2(^2A_2)$ $\Delta H^o_0 = 120.0$ kcal/mol

H – O – N = O protocovalent bond

The protocovalent bond in XONO?

X – ONO

(M = Li, Na, K, CH_3, C_2H_5, F, Cl, Br, I, HO)

S. Berski, Z. Latajka, A.J. Gordon

Electron Localization Function and Electron Localizability Indicator applied to study the bonding in the peroxynitrous acid HOONO.

J.Comput.Chem., 32 (2011) 1528 – 1540

S. Berski, Z. Latajka, A.J. Gordon

Oxygen bound iodine (O-I): The Electron Localization Function (ELF) study on bonding in cis- and trans-IONO.

Chem.Phys.Lett., 506 (2011) 15-21

S. Berski, A.J. Gordon

Comparative density functional theory and post-Hartree-Fock (CCSD, CASSCF) studiem on the electronic structure of halogen nitrites ClONO and BrONO using quantum chemical topology.

J.Chem.Phys., 135 (2011) 094303-1 – 094303-13

Iodine nitrite I-ONO

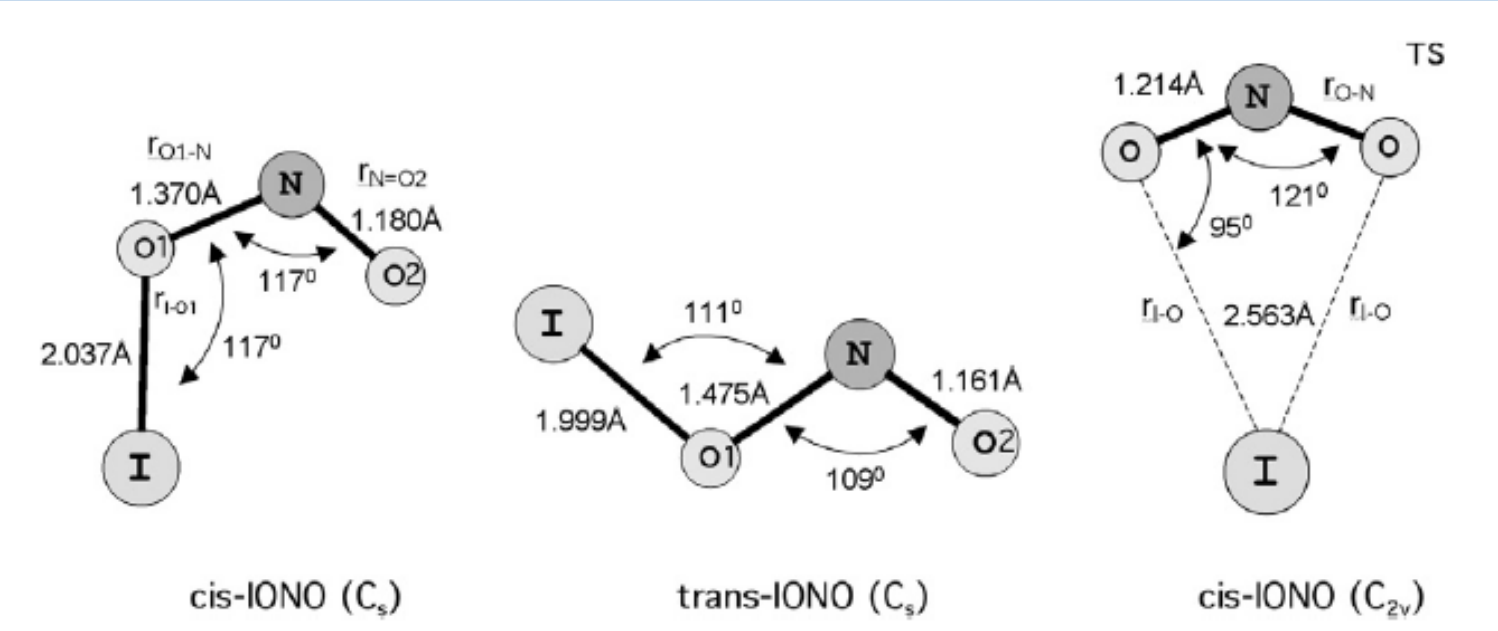

0.0 **4.17 kcal/mol** **8.79 kcal/mol**

S.Berski, Z.Latajka, A.J.Gordon, Chem.Phys.Lett., 506 (2011) 15

I-ONO

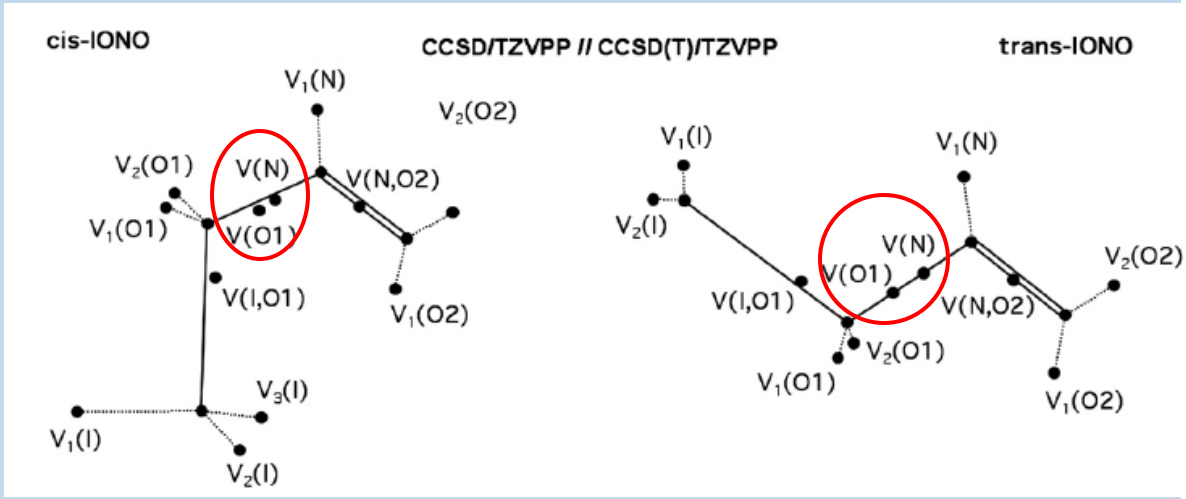

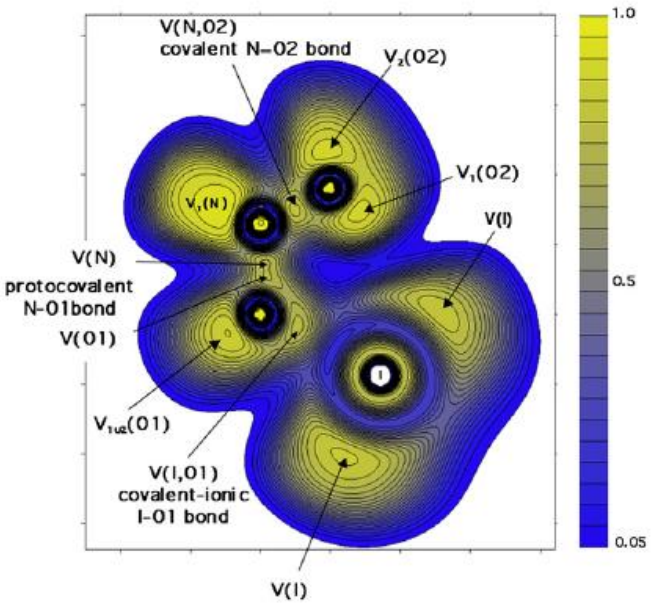

Figure 3. The 2D representation of ELF for the cis-IONO at CCSD/aug-cc-pVTZ// CCSD(T)/aug-cc-pVTZ level.

	cis	trans	bond
V(I,O1)	0.67	0.63	charge shift
V(N,O2)	2.05	2.16	covalent
V(N)	0.63	0.52	protocova-lent
V(O1)	0.47	0.27	

Bond polarity index of t-IONO:

N=O2 0.08 pop. 2.16e (54% O2, 46% N)

I-O1 0.47 pop. 0.63e (73% O1, 27% I)

I-ONO

trans-IONO(^{1}A′) → IO(^{2}) + NO($^2\pi$)
ΔH_0° = 1.26(1.51) **1.43** eV

trans-IONO(^{1}A′) → I(^{2}P) + NO_2($^2A_1$)
ΔH_0° = 0.51(0.76) **0.69** eV

trans-IONO(^{1}A′) → I(^{2}P) + NO_2($^2B_2$)
ΔH_0° = 1.85(2.12) **1.99** eV

trans-IONO(^{1}A′) → I(^{2}P) + NO_2($^2B_1$)
ΔH_0° = 2.14(2.36) **2.44** eV

trans-IONO(^{1}p′) → I(^{2}P) + NO_2(^{2}A″)
ΔH_0° = 2.60(2.88) **2.73** eV

trans-IONO(^{1}A′) → ION(^{1}A′) + O(^{3}P)
ΔH_0° = 3.80(4.06) **3.73** eV

trans-IONO(^{1}A′) → I^+(^{3}P) + NO_2^- ($^1A_1$)
ΔH_0° = 8.89 (9.44) **9.21** eV

trans-IONO(^{1}A′) → I^- (^{1}S) + NO_2^+($^1\Sigma_g$)
ΔH_0° = 7.08(7.39) **6.99** eV

PC

0.79 e

0.63 e

CS

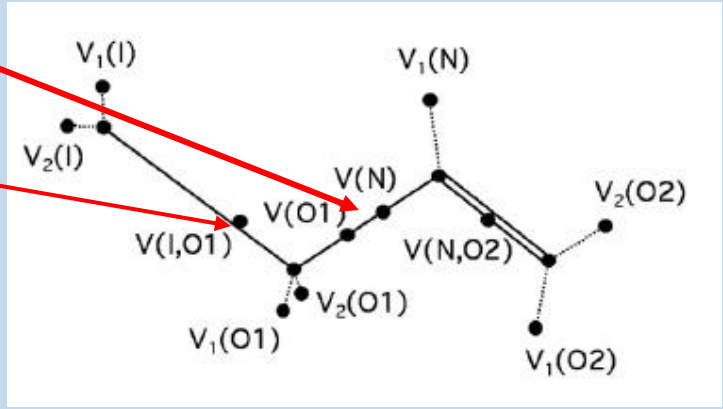

Peroxynitrous acid HOONO

HO – ONO or HOO – NO protocovalent bond?

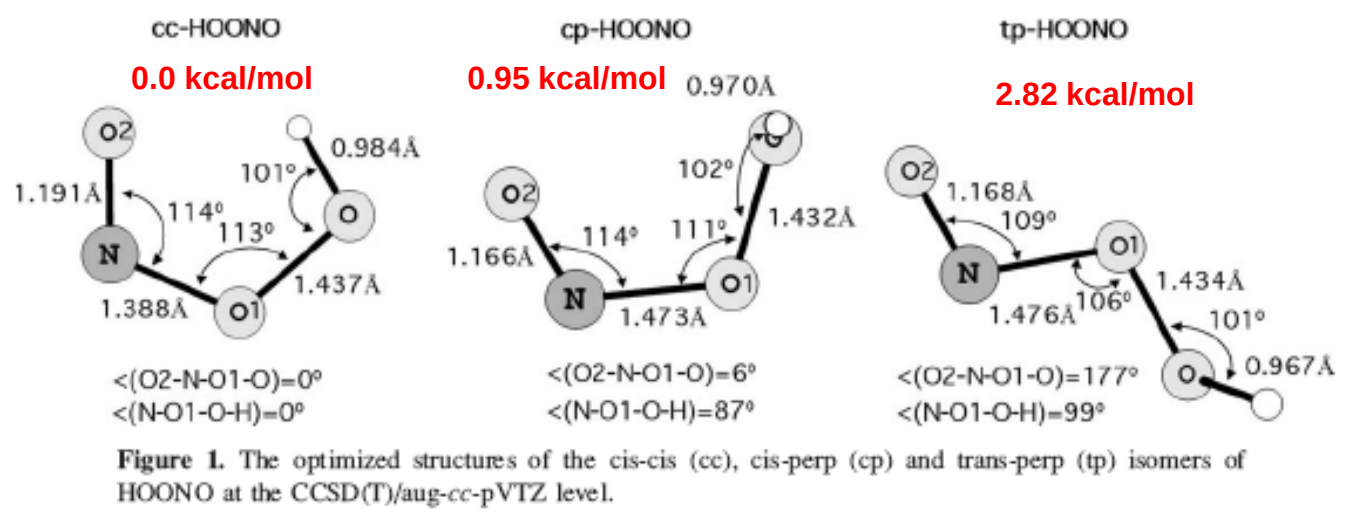

Figure 1. The optimized structures of the cis-cis (cc), cis-perp (cp) and trans-perp (tp) isomers of HOONO at the CCSD(T)/aug-*cc*-pVTZ level.

Rule of the valence octet: H – $\overline{\text{O}}$ – $\overline{\text{O1}}$ – $\overline{\text{N}}$ = $\overline{\text{O2}}$

S.Berski, Z.Latajka, A.J.Gordon, J.Comput.Chem., 32 (2011) 1528

HOONO

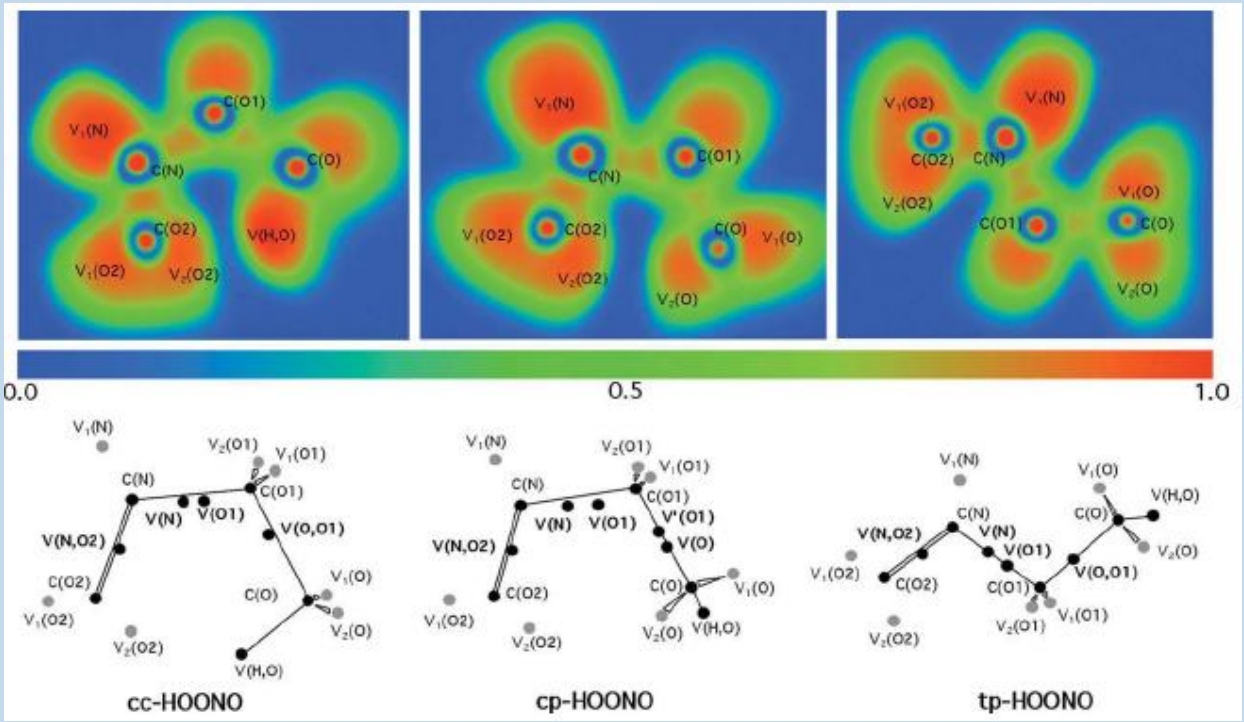

	cc-HOONO	cp-HOONO	tp-HOONO
V(N,O2)	2.00	2.15	2.15
V(N)	0.60	0.54	0.53
V(O1)	0.48	0.29	0.29
V(O,O1)	0.67	-	0.64
V'(O1)	-	0.26	-
V(O)	-	0.35	-

HOONO

Table 5. The splitting the V(A,B) localization basins into atomic contributions A, B $\overline{N}[V(A,B)|A]$ in e calculated for cc, cp, and tp isomers of HOONO at CCSD/aug-*cc*-pVTZ//CCSD(T)/aug-*cc*-pVTZ level.

$\overline{N}[V(A,B)\|A]$	cc	cp	tp
V(N,O2)|N	1.00	1.00	1.01
V(N,O2)|O2	1.00	1.14	1.13
V(N)|N; V(N)|O1	0.57; 0.03	0.53; 0.02	0.51; 0.02
V(O1)|O1; V(O1)|N	0.46; 0.01	0.28; 0.01	0.29; 0.00
V(O,O1)|O	0.25	–	0.28
V(O,O1)|O1	0.42	–	0.36
V′(O1)|O1; V′(O1)|O	–	0.33; 0.01	–
V(O)|O; V(O)|O1	–	0.25; 0.01	–
V(O,H)|O	1.34	1.36	1.35
V(O,H)|H	0.34	0.36	0.36

HOONO

Bonding evolution theory (BET)

the evolution of the V(O,O1) and V(N,O1) basin populations

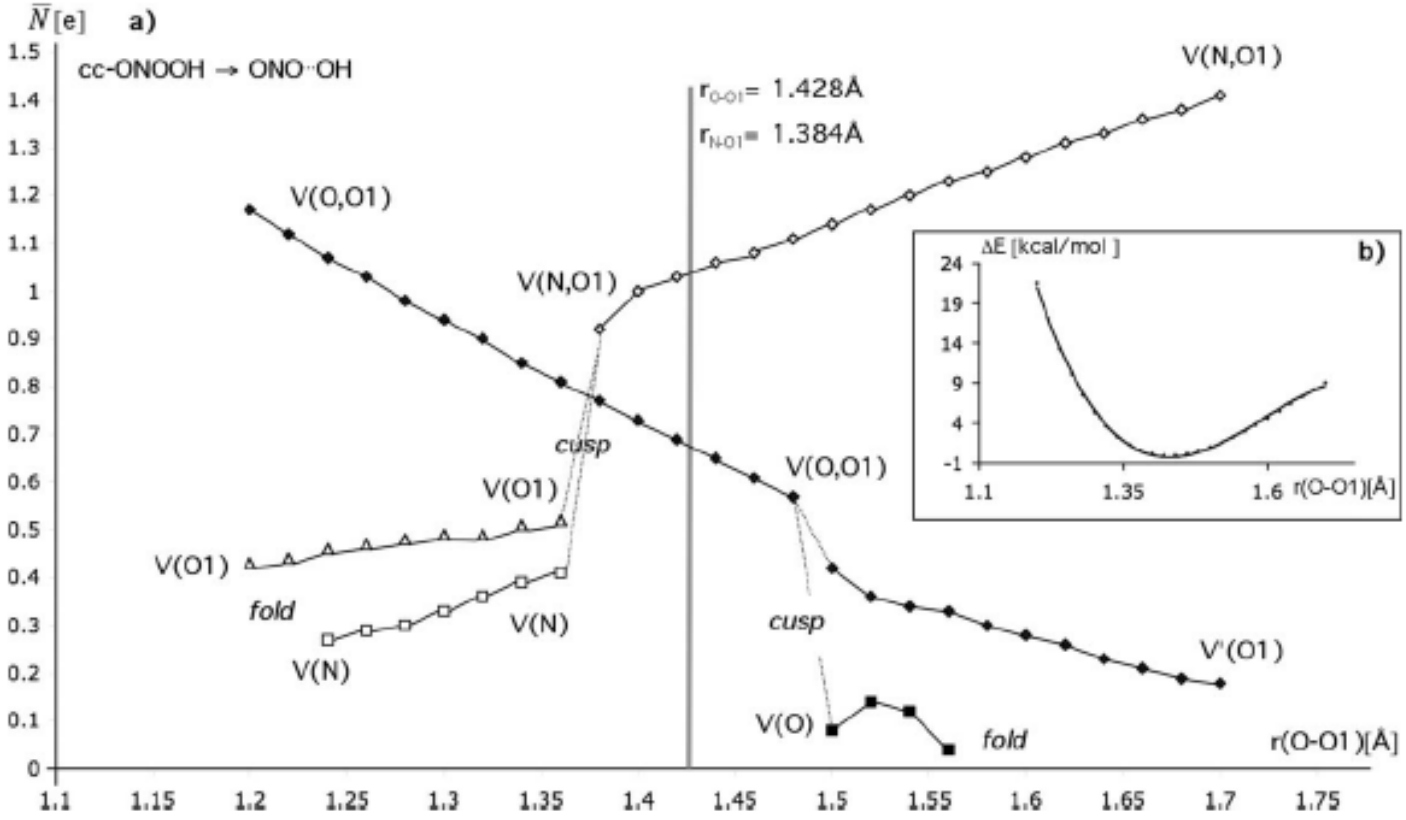

Figure 5. (a) Evolution of the O—O1 and N—O1 bonds during the elongation of the O—O1 bond from 1.2 to 1.7A in cc-HOONO, studied at the B3LYP/aug-*cc*-pVTZ level. The lines linking the points are added to emphasize the trend, (b) MEP calculated for the evolution presented in Figure 5a.

HOONO

1. $HOONO \rightarrow HNO + O_2(^3\Sigma_g^-)$ $\Delta H_0^\circ = 1.23\ (1.18)$ eV
2. $HOONO \rightarrow HNO + O_2(^1\Delta_g)$ $\Delta H_0^\circ = 2.20\ (2.15)$ eV
3. $HOONO \rightarrow OH + NO_2$ $\Delta H_0^\circ = 0.86\ (0.79)$ eV
4. $HOONO \rightarrow HO_2 + NO$ $\Delta H_0^\circ = 1.18\ (1.15)$ eV
5. $HOONO \rightarrow HONO_2$ $\Delta H_0^\circ = -1.26\ (-1.25)$ eV

0.67e CS bond

1.08 e PC bond

Conclusion

Total basin population of the CS/protocovalent bond could be a good indicator of the weakest bond because the covalent bond, which is „partially bonded", is weaker, and with less electron density in the bonding basin, therefore, will break first.

PARTIALLY BONDED MOLECULES AND THEIR TRANSITION TO THE CRYSTALLINE STATE

Kenneth R. Leopold

Advances in Molecular Structure Research
Volume 2, pages 103–127

ISBN: 1-7623-0025-6